Large loss of CO$_2$ in winter observed across the northern permafrost region

Susan M. Natali [1,57]*, Jennifer D. Watts[1,57], Brendan M. Rogers[1], Stefano Potter [1], Sarah M. Ludwig[1], Anne-Katrin Selbmann[2], Patrick F. Sullivan[3], Benjamin W. Abbott [4], Kyle A. Arndt[5], Leah Birch[1], Mats P. Björkman [6], A. Anthony Bloom[7], Gerardo Celis[8], Torben R. Christensen [9], Casper T. Christiansen [10], Roisin Commane [11], Elisabeth J. Cooper [12], Patrick Crill[13], Claudia Czimczik [14], Sergey Davydov[15], Jinyang Du[16], Jocelyn E. Egan[17], Bo Elberling [18], Eugenie S. Euskirchen[19], Thomas Friborg [20], Hélène Genet [19], Mathias Göckede [21], Jordan P. Goodrich[5,22], Paul Grogan[23], Manuel Helbig [24,25], Elchin E. Jafarov [26], Julie D. Jastrow [27], Aram A. M. Kalhori[5], Yongwon Kim [28], John S. Kimball[16], Lars Kutzbach[29], Mark J. Lara [30], Klaus S. Larsen [20], Bang-Yong Lee[31], Zhihua Liu [32], Michael M. Loranty [33], Magnus Lund [9], Massimo Lupascu[34], Nima Madani [7], Avni Malhotra [35], Roser Matamala[27], Jack McFarland[36], A. David McGuire [19], Anders Michelsen [37], Christina Minions[1], Walter C. Oechel[5,38], David Olefeldt [39], Frans-Jan W. Parmentier [40,41], Norbert Pirk [40,41], Ben Poulter [42], William Quinton[43], Fereidoun Rezanezhad[44], David Risk [45], Torsten Sachs [46], Kevin Schaefer [47], Niels M. Schmidt [9], Edward A. G. Schuur [8], Philipp R. Semenchuk[48], Gaius Shaver[49], Oliver Sonnentag[25], Gregory Starr[50], Claire C. Treat [51], Mark P. Waldrop[36], Yihui Wang[5], Jeffrey Welker[52,53], Christian Wille [46], Xiaofeng Xu[5], Zhen Zhang [54], Qianlai Zhuang [55] and Donatella Zona [5,56]

Recent warming in the Arctic, which has been amplified during the winter[1-3], greatly enhances microbial decomposition of soil organic matter and subsequent release of carbon dioxide (CO$_2$)[4]. However, the amount of CO$_2$ released in winter is not known and has not been well represented by ecosystem models or empirically based estimates[5,6]. Here we synthesize regional in situ observations of CO$_2$ flux from Arctic and boreal soils to assess current and future winter carbon losses from the northern permafrost domain. We estimate a contemporary loss of 1,662 TgC per year from the permafrost region during the winter season (October–April). This loss is greater than the average growing season carbon uptake for this region estimated from process models (−1,032 TgC per year). Extending model predictions to warmer conditions up to 2100 indicates that winter CO$_2$ emissions will increase 17% under a moderate mitigation scenario—Representative Concentration Pathway 4.5—and 41% under business-as-usual emissions scenario—Representative Concentration Pathway 8.5. Our results provide a baseline for winter CO$_2$ emissions from northern terrestrial regions and indicate that enhanced soil CO$_2$ loss due to winter warming may offset growing season carbon uptake under future climatic conditions.

Air and soil temperatures in the Arctic are increasing rapidly, with the most severe climate amplification occurring in autumn and winter[1,2]. Although warmer soils decompose more quickly, thus releasing more carbon dioxide (CO$_2$) into the atmosphere, microbial respiration is known to occur even under extremely cold winter conditions (down to approximately −20 °C) in unfrozen microsites, which can persist at subzero soil temperatures[7]. This production and release of CO$_2$ in winter is expected to increase substantially as soils continue to warm and thaw under a warming climate[4,8].

However, it remains uncertain how much CO$_2$ is currently emitted from the permafrost region during winter[9] and how much these emissions might increase in the future[8,10]. Many ecosystem models are not well adapted to simulate respiration from high-latitude soils[5] and may underestimate present and future winter CO$_2$ emissions[6]. Given the limitations in current models, lack of satellite and airborne CO$_2$ data for the Arctic during winter[11], and gaps in spatial coverage of Arctic air monitoring networks[12], in situ CO$_2$ flux observations provide the most direct insight into the state of winter CO$_2$ emissions across the northern permafrost domain.

Studies of winter respiration indicate that the amount of CO$_2$ released during cold periods depends on vegetation type[13], availability of labile carbon substrates[14–16], non-frozen soil moisture[4,7,15,18], microbial community composition and function[19], and snow depth[15,20,21]. However, knowledge of the influence of these drivers on the rates and patterns of winter CO$_2$ flux on a regional scale remains limited[6,9].

Here we present a compilation of in situ CO$_2$ winter flux data for the northern permafrost domain (Fig. 1 and Supplementary Table 1)
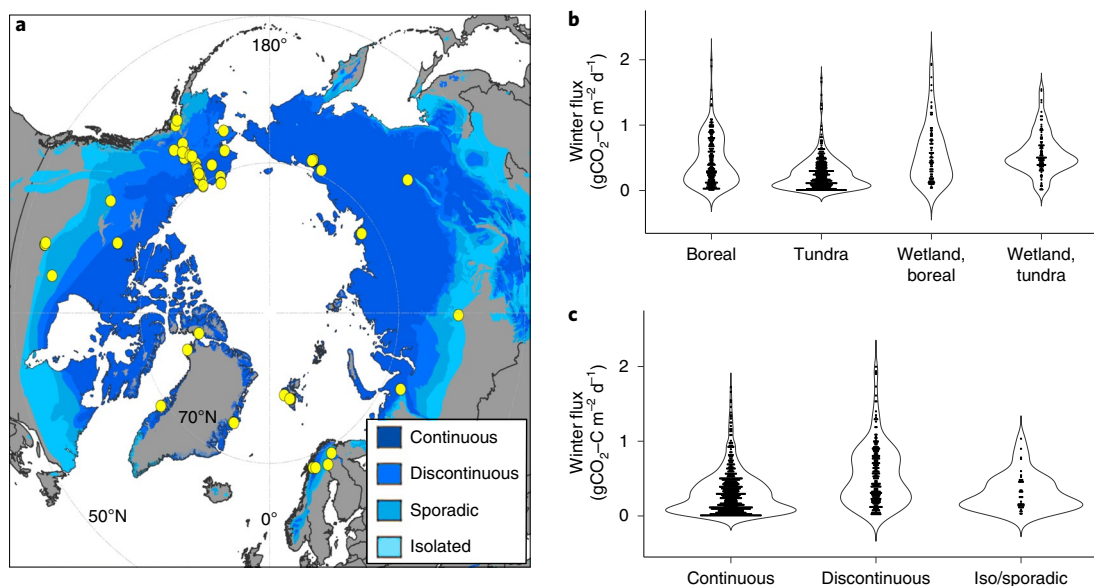
Fig. 1 | Distribution of in situ data included in this winter CO₂ flux synthesis. a, Locations of in situ winter CO₂ flux data (yellow circles) used in our machine learning model, including upland and wetland sites in boreal and tundra biomes located within the northern permafrost region[41]. **b,c**, Violin plots depicting magnitude and distribution density according to vegetation (**b**) and permafrost (**c**) class.

to examine the drivers and magnitude of winter respiration in the Arctic. We define the winter period from October to April—months when the landscape is generally covered by snow and photosynthesis is negligible[22,23]. The dataset represents more than 100 high-latitude sites and comprises more than 1,000 aggregated monthly fluxes. We examined patterns and processes driving winter CO₂ emissions and scaled fluxes to the permafrost domain using a boosted regression tree (BRT) machine learning model based on hypothesized drivers of winter CO₂ flux. Environmental and ecological drivers (for example, vegetation type and productivity, soil moisture and soil temperature) obtained from satellite remote sensing and reanalysis data were used to estimate regional winter CO₂ emissions for contemporary (2003–2017) climatic conditions. We estimated winter fluxes up to 2100 using meteorological and carbon cycle drivers from ensembles of Earth System Model (ESM) outputs for Representative Concentration Pathway (RCP) 4.5 and RCP 8.5 (ref. [24]).

Soil temperature had the strongest influence on winter CO₂ emissions, with fluxes measured at temperatures down to −20 °C (Fig. 2a), in line with results from laboratory incubations (Fig. 2b). This demonstrates that microbial respiration may occur in unfrozen microsites that persist at subzero bulk soil temperatures[18]. Diffusion of stored CO₂ produced during the non-frozen season may have driven some of the emissions measured in winter, but the magnitude of this contribution is unclear. Winter CO₂ emissions increased by a factor of 2.9 (95% credible interval (CI) = (2.1, 4.2)) per 10 °C soil temperature increase (that is, Q10) for in situ fluxes and by a factor of 8.5 (95% CI = (5.0, 14.5)) for CO₂ release from low temperature laboratory incubations. Differences between in situ and laboratory Q10s may reflect site-level differences in environmental drivers other than temperature (in situ and laboratory sites were not fully overlapping), experimental design differences (for example, less restricted diffusion in the laboratory) or variation in the depth of in situ CO₂ production, which can occur throughout the soil profile, relative to the depth of recorded temperature, which tended to be closer to the soil surface (~10 cm).

Air and soil temperatures had the strongest influence on winter flux with a combined relative influence of 32%. Vegetation type (15% relative influence), leaf area index (LAI, 11%), tree cover (10%) and previous summer's gross primary productivity (GPP, 8.5%)

also influenced winter CO₂ emissions (Supplementary Fig. 1). Along with warmer air and soil temperatures in winter and corresponding increases in CO₂ loss, summer GPP has also been increasing in some parts of the northern permafrost region[25]. The positive relationship between GPP and winter CO₂ emissions suggests that increased CO₂ uptake during the growing season may be partially offset by winter CO₂ emissions.

Another important driver of winter respiration was unfrozen water content, which is a function of soil temperature and texture, as finer textured soils contain more unfrozen water than coarse soils for a given subzero temperature[26]. Indirect measurements of unfrozen water availability confirm its importance: soils with low sand and high clay content, which tend to have greater unfrozen microsites, were characterized by higher CO₂ flux rates. Although snow cover is a key driver of winter flux through its impact on ground temperature[27], remote sensing estimates of snow cover were not significant predictors in the model. This may be a result of high uncertainty in regional snow products or because snow depth and density, which are difficult to determine from space using currently available satellite technology[28], have a greater influence on ground temperatures than snow presence alone.

Using our model to assess winter flux for the terrestrial permafrost domain, we estimate approximately 1,662 teragrams of carbon (TgC) per winter released under current climatic conditions (2003–2017), with a corresponding uncertainty of 813 TgC per winter (Supplementary Methods). We observed no temporal trends in winter CO₂ flux during 2003–2017 ($P > 0.1$), which corresponded to the lack of a significant circumpolar trend in the reanalysis winter air or soil temperature data used as model inputs ($P > 0.1$). Although we did not observe region-wide trends during 2003–2017, atmospheric CO₂ enhancements for Alaska[8] and site-level studies from Alaskan tundra[29,30] showed recent increases in winter emissions, which are already shifting some tundra regions from an annual carbon sink to a source.

Our flux estimates are two-fold higher than a previous estimate derived from in situ measurements reported in the Regional Carbon Cycle Assessment and Processes (RECCAP) tundra and northern boreal domain[10], which was based on a much smaller dataset (<20 site-years for winter data). The RECCAP study reported fluxes of
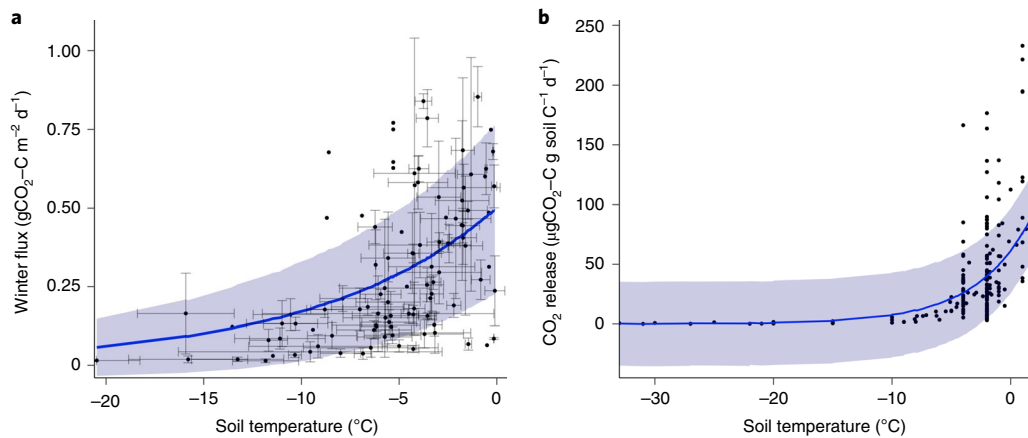
Fig. 2 | Effect of soil temperature on CO$_2$ release from soils. a,b, In situ soil temperature (~10 cm average depth) versus CO$_2$ fluxes (**a**) and CO$_2$ released from laboratory incubations (**b**). Shading represents the standard deviation of an exponential model, which, for in situ fluxes, was fitted to mean CO$_2$ flux from each sample location (symbols shown with standard error). Note that the different soil temperature scales between panels reflect data ranges.

24–41 gC m^{-2} per winter from in situ data, compared to 64 gC m^{-2} per winter, estimated here for the RECCAP region and 98 gC m^{-2} per winter for the full permafrost domain (Supplementary Fig. 2). Our estimate of winter flux agrees more closely with the RECCAP atmospheric inversion estimate (27–81 gC m^{-2} per winter), providing some closure between bottom-up and top-down assessments[6,12].

We then compared our permafrost region flux estimates to winter net ecosystem exchange (NEE) outputs from five process-based terrestrial models and from FluxCom, a global machine learning NEE product[31]. Our winter CO$_2$ flux estimate was generally higher than estimates from these models, which ranged from 377 TgC per winter for FluxCom and from 503 to 1,301 TgC for the process models (mean: 1,008 TgC per winter; Supplementary Fig. 3). Similar variations in carbon budget estimates from terrestrial models have been reported for high-latitude regions[5], which reflects considerable differences in model parameterization of soil temperature, unfrozen water and substrate effects on CO$_2$ production under winter conditions. Some process-based models may underestimate winter CO$_2$ emissions by shutting down respiration at subzero soil temperatures[32] or because they are unable to capture small-scale processes that influence winter flux, such as talik formation and shrub-snow interactions, which are more likely to be captured by in situ measurements.

Combining growing season NEE (−687 to −1,647 TgC per season) and winter NEE derived from the process-based terrestrial models described above results in an estimated annual NEE of −351 to 514 TgC yr^{-1} (−555 for FluxCom; Supplementary Table 2). Because our winter emissions estimate was higher than these process models, we expect that annual CO$_2$ losses may also be higher. For example, if we account for growing season NEE using the process-model estimates, this would yield an average annual CO$_2$ emission of 646 TgC yr^{-1} (range of 15–975) from the permafrost region, based on our estimate of winter CO$_2$ flux.

Our assessment of future winter emissions, obtained by forcing the BRT model with environmental conditions from the Fifth Coupled Model Intercomparison Project (CMIP5) ESM outputs[2], showed significant increases in winter CO$_2$ emissions under both climate scenarios ($P < 0.001$, Fig. 3); however, emissions were substantially lower with climate mitigation in RCP 4.5 than in RCP 8.5. Compared to winter emissions for 2003–2017, there was a 17% projected increase in winter CO$_2$ flux under RCP 4.5 by 2100 (to 1,950 TgC yr^{-1}) and a 41% increase under RCP 8.5 by 2100 (to 2,345 TgC yr^{-1}) (Fig. 4).

The present-day continuous permafrost zone experienced the strongest positive trend in winter CO$_2$ emissions under both

climate scenarios ($P < 0.001$); however, accounting for differences in area, the largest rate of change in winter CO$_2$ emissions occurred across the discontinuous zone (Supplementary Table 3) where soils have warmed rapidly and permafrost has diminished in recent years[33]. The differences in projected changes in winter CO$_2$ emissions among permafrost zones may reflect the influence of latitudinal variation in environmental and ecological variables, including tree cover, dominant vegetation, and soil organic matter content and composition[34].

Increased winter CO$_2$ emissions from our data-driven BRT model were influenced by changes in soil and air temperatures, which increased for soil by 0.04 °C yr^{-1} under RCP 4.5 and by 0.08 °C yr^{-1} under RCP 4.5, and for air by 0.1 °C yr^{-1} under RCP 8.5 (Supplementary Fig. 4). Vegetation leaf area and GPP, both of which were positively related to winter CO$_2$ flux, also significantly increased up to 2100.

From 2018 to 2100, we estimated a cumulative winter flux of 150 PgC for RCP 4.5 and 162 PgC for RCP 8.5. This represents an additional 15 PgC for RCP 4.5 and 27 PgC for RCP 8.5 emitted as a result of climate change compared to the estimated 135 PgC that would be emitted up to 2100 if present (2003–2017) climatic conditions remained constant. These losses are comparable to 70% of the present-day permafrost region near-surface (0–30 cm) soil carbon pool[35]. These projected increases are substantially lower than projections from CMIP5 ESMs, in which winter CO$_2$ emissions from ecosystem respiration for the permafrost region (1,753 ± 1,066 PgC yr^{-1} for 2003–2005) were projected to increase by 2100 by 37% and 86% under RCP 4.5 (2,482 ± 1,403 PgC yr^{-1}) and RCP 8.5 (3,473 ± 1,731 PgC yr^{-1}), respectively (Fig. 4). Our data-driven BRT model may provide more conservative estimates because current in situ observations may not adequately reflect future environmental responses to substantially warmer winter conditions. However, it is also possible that the ESMs are missing stabilizing drivers and mechanisms that might provide negative feedbacks to winter CO$_2$ emissions. We therefore stress the importance of addressing current uncertainties in process-model estimates of growing season and winter CO$_2$ exchange. Given the data limitations during the winter, there is a particular need for long-term monitoring of winter CO$_2$ exchange in permafrost regions to provide key insights into processes that may enhance or mitigate change. As most of the CMIP5 models do not currently include a permafrost component, these data are critical for improving pan-Arctic carbon cycle simulations.

Some of the projected winter CO$_2$ emissions could be offset by plant carbon uptake, which is expected to increase as plants respond favourably to warming and CO$_2$ fertilization[36,37]. In addition, our
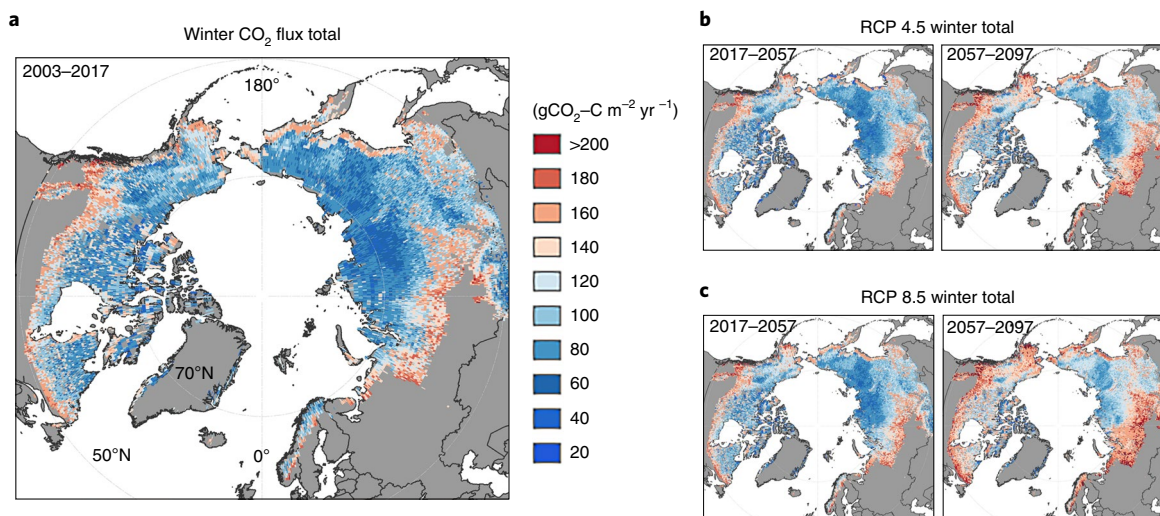
Fig. 3 | Pan-Arctic winter CO₂ emissions under current and future climate scenarios. a, Average annual winter (October–April) CO_2 emissions estimated for the permafrost region for the baseline years 2003–2017. **b,c**, Cumulative winter CO_2 fluxes under RCP 4.5 (**b**) and RCP 8.5 (**c**) scenarios over an 80-year period (2017–2057 and 2057–2097). Fluxes are reported on an annual basis.
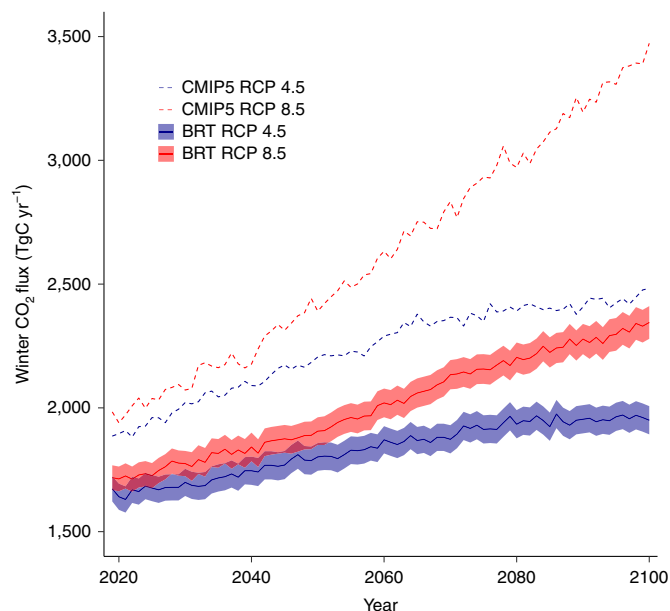

Fig. 4 | Projected annual CO₂ emissions during the winter for the northern permafrost region. Solid lines represent BRT-modelled results up to 2100 under RCP 4.5 (blue solid line) and RCP 8.5 (red solid line), with bootstrapped 95% confidence intervals indicated by shading. For reference, CMIP5 ensemble respiration for RCP 4.5 and 8.5 are also shown (dashed lines).

modelled results do not explicitly account for CO_2 uptake during the shoulder seasons (early and late winter period; for example, October and April), which can occur even under the snowpack[22,23,38] and may increase with climate warming[22]. Our model projections also did not incorporate all changes expected under future climates, such as changes in permafrost distribution, delayed seasonal freeze-up, increased fire frequency, changes in snow cover and distribution, thermokarst frequency and extent, and landscape-level hydrologic changes (for example, lake drainage).

The CO_2 emissions reported here are only part of the winter carbon budget, which also includes substantial methane (CH_4)

emissions from land[17,39] and CO_2 and CH_4 emissions from inland waters[40]. Recent data-derived estimates of high-latitude terrestrial winter CH_4 emissions range from 1.6 TgC yr⁻¹ (land area >60° N)[39] to 9 TgC yr⁻¹ for Arctic tundra[17]. Similar to winter CO_2 emissions, process models underestimated the fraction of annual CH_4 emissions released during the winter[39].

To reduce uncertainty in estimates of current and future emissions, we recommend increased spatial and temporal coverage; coordination and standardization of in situ winter measurements; improvements to regional snow density products and development of remote sensing active sensors that can detect high resolution (<20 km) changes in atmospheric CO_2 concentrations during periods of low to no sunlight, which is a key constraint on monitoring changes in permafrost region carbon cycling. Current rates of winter CO_2 emissions may be offsetting CO_2 uptake by vegetation across the permafrost region. Circumpolar winter CO_2 emissions will likely increase in the near future as temperatures continue to rise; however, this positive feedback on global climate can be mitigated with a reduction of global anthropogenic GHG emissions.

Online content

Any methods, additional references, Nature Research reporting summaries, source data, statements of code and data availability and associated accession codes are available at https://doi.org/10.1038/s41558-019-0592-8.

References

1. Huang, J. Recently amplified Arctic warming has contributed to a continual global warming trend. *Nat. Clim. Change* **7**, 875–879 (2017).
2. Koenigk, T. et al. Arctic Climate Change in 21st century CMIP5 simulations with EC-Earth. *Clim. Dynam.* **40**, 2719–2743 (2013).
3. Cohen, J. et al. Recent Arctic amplification and extreme mid-latitude weather. *Nat. Geosci.* **7**, 627–637 (2014).
4. Schadel, C. et al. Potential carbon emissions dominated by carbon dioxide from thawed permafrost soils. *Nat. Clim. Change* **6**, 950–953 (2016).
5. Fisher, J. B. et al. Carbon cycle uncertainty in the Alaskan Arctic. *Biogeosciences* **11**, 4271–4288 (2014).
6. Commane, R. et al. Carbon dioxide sources from Alaska driven by increasing early winter respiration from Arctic tundra. *Proc. Natl Acad. Sci. USA* **114**, 5361–5366 (2017).

7. Elberling, B. & Brandt, K. K. Uncoupling of microbial CO_2 production and release in frozen soil and its implications for field studies of Arctic C cycling. *Soil Biol. Biochem.* **35**, 263–272 (2003).

8. Schuur, E. A. G. et al. Climate change and the permafrost carbon feedback. *Nature* **520**, 171–179 (2015).

9. Belshe, E. F., Schuur, E. A. G. & Bolker, B. M. Tundra ecosystems observed to be CO_2 sources due to differential amplification of the carbon cycle. *Ecol. Lett.* **16**, 1307–1315 (2013).

10. McGuire, A. D. et al. An assessment of the carbon balance of Arctic tundra: comparisons among observations, process models, and atmospheric inversions. *Biogeosciences* **9**, 3185–3204 (2012).

11. Schimel, D. et al. Observing terrestrial ecosystems and the carbon cycle from space. *Glob. Change Biol.* **21**, 1762–1776 (2014).

12. Parazoo, N., Commane, R., Wofsy, S. C. & Koven, C. D. Detecting regional patterns of changing CO_2 flux in Alaska. *Proc. Natl Acad. Sci. USA* **113**, 7733–7738 (2016).

13. Grogan, P. Cold season respiration across a low Arctic landscape: the influence of vegetation type, snow depth, and interannual climatic variation. *Arct. Antarct. Alp. Res.* **44**, 446–456 (2012).

14. Michaelson, G. J. & Ping, C. L. Soil organic carbon and CO_2 respiration at subzero temperature in soils of Arctic Alaska. *J. Geophys. Res. Atmos.* **108**(D2), 8164 (2005).

15. Rogers, M. C., Sullivan, P. F. & Welker, J. M. Evidence of nonlinearity in the response of net ecosystem CO_2 exchange to increasing levels of winter snow depth in the high Arctic of Northwestern Greenland. *Arct. Antarct. Alp. Res.* **43**, 95–106 (2011).

16. Wang, T. et al. Controls on winter ecosystem respiration in temperate and boreal ecosystems. *Biogeosciences* **8**, 2009–2025 (2011).

17. Zona, D. et al. Cold season emissions dominate the Arctic tundra methane budget. *Proc. Natl Acad. Sci. USA* **113**, 40–45 (2016).

18. Schaefer, K. & Jafarov, E. A parameterization of respiration in frozen soils based on substrate availability. *Biogeosciences* **13**, 1991–2001 (2016).

19. Monson, R. et al. Winter forest soil respiration controlled by climate and microbial community composition. *Nature* **439**, 711–714 (2006).

20. Welker, J. M., Fahnestock, J. T. & Jones, M. H. Annual CO_2 flux in dry and moist Arctic tundra: field responses to increases in summer temperatures and winter snow depth. *Climatic Change* **44**, 139–150 (2000).

21. Natali, S. M. et al. Effects of experimental warming of air, soil and permafrost on carbon balance in Alaskan tundra. *Glob. Change Biol.* **17**, 1394–1407 (2011).

22. Webb, E. E. et al. Increased wintertime CO_2 loss as a result of sustained tundra warming. *Biogeosciences* **121**, 1–17 (2016).

23. Christiansen, C. T., Schmidt, N. M. & Michelsen, A. High Arctic dry heath CO_2 exchange during the early cold season. *Ecosystems* **15**, 1083–1092 (2012).

24. Knutti, R., Masson, D. & Gettelman, A. Climate model genealogy: generation CMIP5 and how we got there. *Geophys. Res. Lett.* **40**, 1194–1199 (2013).

25. Forkel, M. et al. Enhanced seasonal CO_2 exchange caused by amplified plant productivity in northern ecosystems. *Science* **351**, 696–699 (2016).

26. Tucker, C. Reduction of air- and liquid water-filled soil pore space with freezing explains high temperature sensitivity of soil respiration below 0 °C. *Soil Biol. Biochem.* **78**, 90–96 (2014).

27. Loranty, M. M. et al. Reviews and syntheses: changing ecosystem influences on soil thermal regimes in northern high-latitude permafrost regions. *Biogeosciences* **15**, 5287–5313 (2018).

28. Witze, A. Snow-sensing fleet to unlock water's icy secrets. *Nature* **532**, 17 (2016).

29. Natali, S. M. et al. Permafrost thaw and soil moisture driving CO_2 and CH_4 release from upland tundra. *J. Geophys. Res. Biogeosci.* **120**, 525–537 (2015).

30. Euskirchen, E. S., Bret-Harte, M. S., Shaver, G. R., Edgar, C. W. & Romanovsky, V. E. Long-term release of carbon dioxide from Arctic tundra ecosystems in Alaska. *Ecosystems* **20**, 960–974 (2017).

31. Tramontana, G. et al. Predicting carbon dioxide and energy fluxes across global FLUXNET sites with regression algorithms. *Biogeosciences* **13**, 4291–4313 (2016).

32. Koven, C. D. et al. Permafrost carbon-climate feedbacks accelerate global warming. *Proc. Natl Acad. Sci. USA* **108**, 14769–14774 (2011).

33. Slater, A. G. & Lawrence, D. M. Diagnosing present and future permafrost from climate models. *J. Clim.* **26**, 5608–5623 (2013).

34. Vanhala, P. et al. Temperature sensitivity of soil organic matter decomposition in southern and northern areas of the boreal forest zone. *Soil Biol. Biochem.* **40**, 1758–1764 (2008).

35. Hugelius, G. E. A. Estimated stocks of circumpolar permafrost carbon with quantified uncertainty ranges and identified data gaps. *Biogeosciences* **11**, 6573–6593 (2014).

36. McGuire, A. D. et al. Dependence of the evolution of carbon dynamics in the northern permafrost region on the trajectory of climate change. *Proc. Natl Acad. Sci. USA* **115**, 3882–3887 (2018).

37. Qian, H., Joseph, R. & Zeng, N. Enhanced terrestrial carbon uptake in the northern high latitudes in the 21st century from the Coupled Carbon Climate Model Intercomparison Project model projections. *Glob. Change Biol.* **16**, 641–656.

38. Starr, G. O. et al. Photosynthesis of Arctic evergreens under snow: implications for tundra ecosystem carbon balance. *Ecology* **84**, 1415–1420 (2003).

39. Treat, C. C., Bloom, A. A. & Marushchak, M. E. Nongrowing season methane emissions: a significant component of annual emissions across northern ecosystems. *Glob. Change Biol.* **24**, 3331–3343 (2018).

40. Walter Anthony, K. et al. 21st-century modeled permafrost carbon emissions accelerated by abrupt thaw beneath lakes. *Nat. Commun.* **9**, 3262 (2018).

41. *Circum-Arctic Map of Permafrost and Ground-Ice Conditions, Version 2* (National Snow & Ice Data Center, 2002); https://nsidc.org/data/ggd318

Author contributions

S.M.N., J.D.W. and B.M.R conceived the work. B.W.A., G.C., C.T.C., H.G., E.E.J., M.M.L., S.M.L., M.L., A.M., C.M., S.M.N., F.R., B.M.R., K.S., A.-K.S., C.C.T., Y.W. and X.X. extracted unpublished data. K.A.A, M.P.B, G.C, T.R.C, E.J.C, C.T.C., S.D., J.D., J.E.E., B.E., E.S.E., T.F., M.G., J.P.G., P.G., M.H., J.D.J., A.A.M.K., Y.K., L.K., K.S.L., M.L., R.M., J.M., A.M., S.M.N., W.C.O., F.-J.W.P., N.P., W.Q., D.R., T.S., N.M.S., E.A.G.S, P.R.S., O.S., P.F.S., M.P.W., C.W. and D.Z. provided unpublished or raw data. L.B., A.A.B., J.D., J.S.K., Z.L., N.M., A.D.M., B.P. and Z.Z. provided modelled data and results. S.M.L., C.M., S.M.N., S.P. and J.D.W. prepared tables and figures. G.C., H.G., M.J.L., M.M.L., S.M.L, S.M.N., S.P., B.M.R., P.F.S. and J.D.W. performed statistical analyses, including BRT modelling. S.P., B.M.R. and J.W. led the BRT upscaling or projection analyses. All authors contributed to data interpretation and preparation of manuscript text.

Competing interests

The author declare no competing interests.

Additional information

Supplementary information is available for this paper at https://doi.org/10.1038/s41558-019-0592-8.

Correspondence and requests for materials should be addressed to S.M.N.

Peer review information *Nature Climate Change* thanks John Campbell and the other, anonymous, reviewer(s) for their contribution to the peer review of this work.

Reprints and permissions information is available at www.nature.com/reprints.

Publisher's note Springer Nature remains neutral with regard to jurisdictional claims in published maps and institutional affiliations.

[1]Woods Hole Research Center, Falmouth, MA, USA. [2]University of Bayreuth, Bayreuth, Germany. [3]Environment and Natural Resources Institute, University of Alaska, Anchorage, AK, USA. [4]Department of Plant and Wildlife Sciences, Brigham Young University, Provo, UT, USA. [5]Department of Biology, San Diego State University, San Diego, CA, USA. [6]Department of Earth Sciences, University of Gothenburg, Göteborg, Sweden. [7]Jet Propulsion Laboratory, California Institute of Technology, Pasadena, CA, USA. [8]Center for Ecosystem Science and Society, Northern Arizona University, Flagstaff, AZ, USA. [9]Department of Bioscience, Arctic Research Centre, Aarhus University, Roskilde, Denmark. [10]NORCE Norwegian Research Centre, Bjerknes Centre for Climate Research, Bergen, Norway. [11]Department of Earth and Environmental Sciences of Lamont-Doherty Earth Observatory, Columbia University, Palisades, NY, USA. [12]Department of Arctic and Marine Biology, Faculty of Biosciences, Fisheries and Economics, UiT The Arctic University of Norway, Tromsø, Norway. [13]Department of Geological Sciences and Bolin Centre for Climate Research, Stockholm University, Stockholm, Sweden. [14]Earth System Science, University of California, Irvine, CA, USA. [15]Northeast Science Station, Pacific Geographical Institute, Cherskii, Russia. [16]Numerical Terradynamic Simulation Group, W.A. Franke College of Forestry & Conservation, University of Montana, Missoula, MT, USA. [17]Department of Earth Sciences, Dalhousie University, Halifax, Nova Scotia, Canada. [18]Center for Permafrost, Department of Geosciences and Natural Resource Management, University of Copenhagen, Copenhagen, Denmark. [19]Institute of Arctic Biology, University of Alaska Fairbanks, Fairbanks, AK, USA. [20]Department of Geosciences and Natural Resource Management, University of Copenhagen, Copenhagen, Denmark. [21]Max Planck Institute for Biogeochemistry, Jena, Germany. [22]Scripps Institution of Oceanography, University of California San Diego, La Jolla, CA, USA. [23]Department of Biology, Queen's University, Kingston, Ontario, Canada. [24]School of Geography and Earth Sciences, McMaster University, Hamilton, Ontario, USA. [25]Department of Geography & Center for Northern Studies, University of Montreal, Montreal, Quebec, Canada. [26]Earth and Environmental Sciences Division, Los Alamos National Laboratory, Los Alamos, NM, USA. [27]Environmental Science Division, Argonne National Laboratory, Argonne, IL, USA. [28]International Arctic Research Center, University of Alaska Fairbanks, Fairbanks, AK, USA. [29]Institute of Soil Science, University of Hamburg, Hamburg, Germany. [30]Department of Plant Biology, University of Illinois, Urbana, IL, USA. [31]Korea Polar Research Institute, Incheon, Republic of Korea. [32]Chinese Academy of Sciences Key Laboratory of Forest Ecology and Management, Institute of Applied Ecology, Chinese Academy of Sciences, Shenyang, China. [33]Department of Geography, Colgate University, Hamilton, NY, USA. [34]Department of Geography, National University of Singapore, Singapore, Singapore. [35]Department of Earth System Science, Stanford University, Stanford, CA, USA. [36]Geology, Minerals, Energy, and Geophysics Science Center, US Geological Survey, Menlo Park, CA, USA. [37]Department of Biology, University of Copenhagen, Copenhagen, Denmark. [38]University of Exeter, Exeter, UK. [39]Department of Renewable Resources, University of Alberta, Edmonton, Alberta, Canada. [40]Department of Geosciences, University of Oslo, Oslo, Norway. [41]Department of Physical Geography and Ecosystem Science, Lund University, Lund, Sweden. [42]Biospheric Sciences Laboratory, NASA Goddard Space Flight Center, Greenbelt, MD, USA. [43]Wilfrid Laurier University, Waterloo, Ontario, Canada. [44]Ecohydrology Research Group, Water Institute and Department of Earth & Environmental Sciences, University of Waterloo, Waterloo, Ontario, Canada. [45]St. Francis Xavier University, Antigonish, Nova Scotia, Canada. [46]GFZ German Research Centre for Geosciences, Telegrafenberg, Potsdam, Germany. [47]Cooperative Institute for Research in Environmental Science, National Snow and Ice Data Center, University of Colorado, Boulder, CO, USA. [48]Department of Botany and Biodiversity Research, University of Vienna, Vienna, Austria. [49]The Ecosystems Center, Marine Biological Laboratory, Woods Hole, MA, USA. [50]Department of Biological Sciences, University of Alabama, Tuscaloosa, AL, USA. [51]Department of Environmental and Biological Science, University of Eastern Finland, Kuopio, Finland. [52]Department of Biological Sciences, University of Alaska Anchorage, Anchorage, AK, USA. [53]Ecology and Genetics Research Unit, University of Oulu, Oulu Finland and UArctic, Rovaniemi, Finland. [54]Department of Geographical Sciences, University of Maryland, College Park, MD, USA. [55]Department of Earth, Atmospheric and Planetary Sciences, Purdue University, West Lafayette, IN, USA. [56]University of Sheffield, Sheffield, UK. [57]These authors contributed equally: Susan. M. Natali, Jennifer D. Watts. *e-mail: snatali@whrc.org

Methods

Data overview. We compiled a dataset of in situ winter season (October–April) CO_2 emissions and potential driving variables from sites within the northern permafrost zone[41]. The synthesized dataset included 66 published studies and 21 unpublished studies (Supplementary Table 1) conducted at 104 sites (that is, sample areas with unique geographic coordinates) and in 152 sampling locations (that is, different locations within a site as distinguished by vegetation type, landscape position, and so on). Sites spanned boreal and tundra landcover classes (Supplementary Fig. 5 and Table 4) in continuous permafrost ($n = 69$), discontinuous ($n = 24$) and isolated/sporadic ($n = 11$) permafrost zones (Fig. 1). Data were aggregated at the monthly level; however, the number of measurements per month varied among studies. The dataset included more than 1,000 site–month flux measurements. We also extracted CO_2 data from incubations of permafrost region soils (Supplementary Table 5) to compare their temperature response functions (Q10) with Q10 derived from the synthesized in situ flux data. Further details of data extraction and Q10 calculations can be found in the Supplementary Methods.

Data extraction and geospatial data. We extracted data from regional gridded geospatial products, including climatological data, soil temperature and moisture, snow water equivalent, soil carbon stocks and texture, permafrost status, vegetation cover, and proxies of vegetation growth and productivity (for example, enhanced vegetation index, LAI, GPP). See Supplementary Methods for further description and data sources. All geospatial data were re-gridded to the National Snow & Ice Data Center Equal Area Scalable Earth 2.0 format[42] at a 25-km spatial resolution before the CO_2 flux upscaling and simulations.

BRT analysis. We used BRT analysis to model drivers of winter CO_2 emissions and to upscale emissions to the northern permafrost region under current and future climate scenarios. The BRT model was fit in R[43] using gbm package v.2.1.1 (ref. [44]) and using code adapted from ref. [45]. The BRT model was fitted with the following metaparameters: Gaussian error distribution, bag-fraction (that is, proportion of data used in each iteration) of 0.5, learning rate (contribution of each tree to the final model) of 0.005 and a tree complexity (maximum level of interactions) of 2. We used ten-fold cross-validation (CV) to determine the optimal number of trees to achieve minimum predictive error and to fit the final model to the data.

We used geospatial data as explanatory variables in our BRT model (see Supplementary Methods for full description of input data). We removed highly correlated variables from the models (Spearman $\rho = 0.7$), retaining the variable within each functional category (for example, air temperature) that had the highest correlation with winter flux. We further reduced the model by removing variables in reverse order of their relative influence, until further removal resulted in a 2% average increase in predictive deviance. We compared this model to one in which we included site-level in situ data as explanatory variables. We used the geospatial model because it allowed us to upscale results and because the percentage deviance (Supplementary Table 6) and driving variables (Supplementary Fig. 1) were similar between models.

We assessed BRT model performance using the (1) correlation between predicted and observed values using the CV data (that is, data withheld from model fitting), hereafter referred to as the CV correlation and (2) deviance explained by the model over the evaluation dataset (that is, CV data), which was calculated as % deviance = (CV null deviance – CV residual deviance)/CV null deviance × 100. Further details of the BRT models can be found in the Supplementary Methods.

We obtained an estimate of model uncertainty by first obtaining the average internal root mean squared error ($0.21\,\mathrm{gC\,m^{-2}\,d^{-1}}$) for the ensemble of BRTs. We then made the assumption that this error applied equally to all grid cell areas within the domain. Scaling this error to the full domain ($16.95 \times 10^6\,\mathrm{km^2}$) and by the total number of days for the winter (October–April) provided us with a winter flux error of 813 TgC per winter.

Spatial and temporal domain for mapping. We scaled the modelled flux data to the northern permafrost land area ≥49° N (ref. [41]), which comprises $16.95 \times 10^6\,\mathrm{km^2}$ of tundra and boreal lands (but excluding glaciers, ice sheets and barren lands; Fig. 1) with lake area removed. We defined the winter period as October to April. Because the climate within this timeframe varies substantially across the permafrost zone, this month-based definition, although temporally consistent, may include some areas that are influenced by climate that would fall outside the expected winter temperature ranges. In a separate approach (see Supplementary Methods), we therefore defined winter based on soil temperature, but we did not find substantial differences in regional flux budgets when using the two approaches (temperature-defined winter flux was approximately 5% higher, 1,743 TgC, than when using the month-based winter period).

Spatial upscaling of fluxes. The BRT model was applied at a monthly time step from 2003 to 2017. For each month, the map predictions were applied to a raster stack of input predictors using the R dismo package[46] for interface with the gbm

package and the raster v.2.6–7 predict function for geospatial model applications. A n.tree (number of trees) of 1,000 was selected for each model run. Output monthly mean estimates of daily CO_2 flux ($\mathrm{gCO_2-C\,m^{-2}\,d^{-1}}$) were generated for each 25-km grid cell. Total pan-Arctic CO_2 flux was obtained on a monthly basis by first calculating the terrestrial area for each grid cell by subtracting lake fractions (moderate resolution imaging spectroradiometer satellite product MOD44W) from each grid cell area. The fluxes were then scaled according to days per month and terrestrial area to obtain per grid cell totals.

We analysed the pan-Arctic flux data for annual temporal trends using the nonparametric Mann–Kendall test, which was run in the R zyp package[47] with pre-whitening (Yue and Pilon method) to remove autocorrelation. We report Kendall's correlation coefficient, τ, to describe the strength of the time-series and the Theil–Sen slope to describe trends over time.

Comparison of BRT estimates with process-based models. We compared our regional winter flux estimates to (1) outputs from five process-based terrestrial models estimated for the northern permafrost domain: National Center for Atmospheric Research Community Land Model (NCAR CLM) v.4.5; NCAR CLM v.5; Lund–Potsdam–Jena Dynamic Global Vegetation Model (LPJ-DGVM), Wald Schnee und Landscraft version (LPJ-wsl); CARbon DAta MOdel FraMework (CARDAMOM); and the NASA SMAP Level 4 Carbon (L4C) v.3 product; (2) estimates for the northern permafrost domain derived from FluxCom, a global gridded machine learning NEE product and (3) four process-based terrestrial models and eight atmospheric inversion models from the high-latitude model intercomparison for the RECCAP tundra and northern boreal domain[10] (see Supplementary Methods for further description of these models).

Projected CO_2 flux. Inputs for the BRT model of future scenarios of winter CO_2 flux were obtained from ensembles of ESM outputs from the Fifth Coupled Model Intercomparison Project (CMIP5) for RCP 4.5 and RCP 8.5 (ref. [2]). Inputs included (1) annual GPP, (2) mean annual summer LAI (July and August), (3) mean summer soil moisture (June, July, August), (4) mean monthly soil moisture, (5) mean monthly near-surface (2 m) air temperature and (6) mean monthly soil temperature (layer 1) (Supplementary Table 7). Ensemble mean RCP 4.5 and RCP 8.5 predictor fields were bias-corrected using the delta, or perturbation method[48], based on historic ESM outputs and observed historical data and re-projected to the Equal Area Scalable Earth (EASE) 2.0 format of 25-km grids.

In addition to the $0.21\,\mathrm{gC\,m^{-2}\,d^{-1}}$ error obtained based on the BRT model root mean squared error, we used the outcome from bootstrapped BRT model simulations to estimate additional, inherit prediction variability in the machine learning outcomes for current and future CO_2 emissions[49] (see Supplementary Information).

For the CMIP5 RCP 4.5 and RCP 8.5 simulations of respiration, we used an r1i1p1 ensemble mean from 15 models (see Supplementary Information).

Reporting Summary. Further information on research design is available in the Nature Research Reporting Summary linked to this article.

Data availability

Data are archived and freely available at the Oak Ridge National Laboratory Distributed Active Archive Center. The synthesis dataset is available at https://doi.org/10.3334/ORNLDAAC/1692. Monthly carbon flux maps (25 km, October–April, 2003–2018; 2018–2100 for RCP 4.5 and RCP 8.5) are available at https://doi.org/10.3334/ORNLDAAC/1683.

References

42. Brodzik, M. J., Billingsley, B., Haran, T., Raup, B. & Savoie, M. H. EASE-Grid 2.0: incremental but significant improvements for Earth-gridded data sets. *ISPRS Int. J. Geoinf.* **1**, 32–45 (2012).
43. R Core Team *R: A Language and Environment for Statistical Computing* (R Foundation for Statistical Computing, 2016).
44. Ridgeway, G. Generalized Boosted Models: A guide to the gbm package. R version 2.1.5 (2007).
45. Elith, J., Leathwick, J. R. & Hastie, T. A working guide to boosted regression trees. *J. Anim. Ecol.* **77**, 802–813 (2008).
46. Hijmans, R. J., Phillips, S., Leathwick, J. & Elith, J. Dismo: Species distribution modelling. R version 1.1-4 (2017).
47. Bronaugh, D. W. Zyp: Zhang + Yue-Pilon trends package. R version 0.10-1.1 (2017).
48. Rogers, B. M., et. al. Impacts of climate change on fire regimes and carbon stocks of the US Pacific Northwest. *J. Geophys. Res. Biogeosci.* **116**, G03037 (2011).
49. Leathwick, J. R., Elith, J., Francis, M. P., Hastie, T. & Taylor, P. Variation in demersal fish species richness in the oceans surrounding New Zealand: an analysis using boosted regression trees. *Mar. Ecol. Prog. Ser.* **321**, 267–281 (2006).

Corresponding author(s): Susan Natali

Last updated by author(s): Aug 30, 2019

Reporting Summary

Nature Research wishes to improve the reproducibility of the work that we publish. This form provides structure for consistency and transparency in reporting. For further information on Nature Research policies, see Authors & Referees and the Editorial Policy Checklist.

Statistics

For all statistical analyses, confirm that the following items are present in the figure legend, table legend, main text, or Methods section.

n/a	Confirmed	
☒	☐	The exact sample size (*n*) for each experimental group/condition, given as a discrete number and unit of measurement
☐	☒	A statement on whether measurements were taken from distinct samples or whether the same sample was measured repeatedly
☐	☒	The statistical test(s) used AND whether they are one- or two-sided *Only common tests should be described solely by name; describe more complex techniques in the Methods section.*
☒	☐	A description of all covariates tested
☐	☒	A description of any assumptions or corrections, such as tests of normality and adjustment for multiple comparisons
☐	☒	A full description of the statistical parameters including central tendency (e.g. means) or other basic estimates (e.g. regression coefficient) AND variation (e.g. standard deviation) or associated estimates of uncertainty (e.g. confidence intervals)
☐	☒	For null hypothesis testing, the test statistic (e.g. *F*, *t*, *r*) with confidence intervals, effect sizes, degrees of freedom and *P* value noted *Give P values as exact values whenever suitable.*
☐	☒	For Bayesian analysis, information on the choice of priors and Markov chain Monte Carlo settings
☐	☒	For hierarchical and complex designs, identification of the appropriate level for tests and full reporting of outcomes
☒	☐	Estimates of effect sizes (e.g. Cohen's *d*, Pearson's *r*), indicating how they were calculated

Our web collection on statistics for biologists contains articles on many of the points above.

Software and code

Policy information about availability of computer code

Data collection	We use PlotDigitizer to extract data from published figures.
Data analysis	The Boosted Regression Tree model was fit in R (R Team 2016) using 'gbm' package version 2.1.1 (Ridgeway 2007), and using code adapted from Elith et al. (2008).

For manuscripts utilizing custom algorithms or software that are central to the research but not yet described in published literature, software must be made available to editors/reviewers. We strongly encourage code deposition in a community repository (e.g. GitHub). See the Nature Research guidelines for submitting code & software for further information.

Data

Policy information about availability of data

All manuscripts must include a data availability statement. This statement should provide the following information, where applicable:

- Accession codes, unique identifiers, or web links for publicly available datasets
- A list of figures that have associated raw data
- A description of any restrictions on data availability

Data are archived and freely available at the ORNL Distributed Active Archive Center (DAAC). The synthesis dataset is available at https://doi.org/10.3334/ORNLDAAC/1692. Monthly carbon flux maps (25 km, October-April, 2003-2018; 2018-2100 for RCP 4.5 and RCP 8.5) are available at https://doi.org/10.3334/ORNLDAAC/1683.

Field-specific reporting

Please select the one below that is the best fit for your research. If you are not sure, read the appropriate sections before making your selection.

☐ Life sciences   ☐ Behavioural & social sciences   ☒ Ecological, evolutionary & environmental sciences

For a reference copy of the document with all sections, see nature.com/documents/nr-reporting-summary-flat.pdf

Ecological, evolutionary & environmental sciences study design

All studies must disclose on these points even when the disclosure is negative.

Study description	This study assessed current and future winter CO2 losses from the northern permafrost domain using a new compilation of in situ CO2 winter flux data. We examined patterns and processes driving winter CO2 emissions and scaled fluxes to the permafrost domain using a boosted regression tree (BRT) machine learning model based on hypothesized drivers of winter CO2 flux.
Research sample	The synthesis dataset used in this study represents more than 100 high latitude sites and comprises more than 1000 aggregated monthly fluxes. The synthesized dataset included 66 published studies and 21 unpublished studies conducted at 104 sites (i.e., sample areas with unique geographic coordinates) and in 152 sampling locations (i.e., different locations within a site as distinguished by vegetation type, landscape position, etc.). Sites spanned boreal and tundra landcover classes in continuous permafrost (n=69), discontinuous (n=24), and isolated/sporadic (n=11) permafrost zones. Data were aggregated at the monthly level; however, the number of measurements per month varied among studies. We synthesized data across studies and measurement methods because of the relatively sparse sampling and representation provided by any one study alone.
Sampling strategy	We synthesized all available winter flux data from the permafrost region. We chose this approach because of the relatively small sample sizes provided by any one study alone and because we wanted to upscale our results to the pan-Arctic region.
Data collection	This study synthesized previously collected data. Data were extracted from publications (using PlotDigitizer software for figures) and obtained directly from data providers in the case of unpublished data. We used a Web of Science search and surveys of the community (through the Permafrost Carbon Network) to identify data to include in this synthesis. Data were compiled by several co-authors, but the final data set was checked by the lead author.
Timing and spatial scale	The data includes sites across the norther permafrost domain and data collected from 1989 through 2017. Data were aggregated at the monthly level, or seasonally when monthly data were not available; the number of measurements per month varied among studies.
Data exclusions	We excluded modeled CO2 flux data from the synthesis dataset, but included gap-filled data when the gap-filling model was based on data collected during the winter. We also excluded data that were averaged across multiple years. For eddy covariance data, we used fluxes of net ecosystem exchange (NEE) or, when fluxes were partitioned, ecosystem respiration, which were essentially the same during the winter. When a monthly winter flux was negative (i.e., signifying CO2 uptake), we excluded that month from the analysis. Negative winter fluxes can occur under low CO2 flux conditions and/or due to instrument-related error, particularly with open-path eddy covariance systems.

We filtered out monthly average CO2 fluxes that were anomalously high (> 2 g C m-2 day-1; n=4, 0.4% of data) and negative/zero fluxes (< 0.001 g C m-2 day-1; n=5). To minimize the contribution from autotrophic CO2 exchange, we filtered fluxes measured when in situ air temperatures were greater than 5° C and soil temperatures (0-25 cm) were greater than -1°C and using a measurement method that included aboveground vegetation (e.g., eddy covariance; n=4); we retained data with > 5° C air temperatures and > -1° C soil temperature when fluxes were measured below the snowpack. We excluded all data with reported soil temperatures greater than 2° C. Data were also filtered to reduce model overfitting resulting from limited data. |
Reproducibility	This is not relevant to this study because we used a machine learning approach to identify drivers of winter flux and upscale fluxes based on the synthesis dataset described above. All data and code are being archived, so the results can be reproduced.
Randomization	This is not relevant to this study because we used a machine learning approach to identify drivers of winter flux and upscale fluxes based on the synthesis dataset described above.
Blinding	This is not relevant to this study because we used a machine learning approach to identify drivers of winter flux and upscale fluxes based on the synthesis dataset described above.

Did the study involve field work?   ☐ Yes   ☒ No

Reporting for specific materials, systems and methods

We require information from authors about some types of materials, experimental systems and methods used in many studies. Here, indicate whether each material, system or method listed is relevant to your study. If you are not sure if a list item applies to your research, read the appropriate section before selecting a response.

Materials & experimental systems

n/a	Involved in the study
☒	Antibodies
☒	Eukaryotic cell lines
☒	Palaeontology
☒	Animals and other organisms
☒	Human research participants
☒	Clinical data

Methods

n/a	Involved in the study
☒	ChIP-seq
☒	Flow cytometry
☒	MRI-based neuroimaging